ISSN: 0974-5823 Vol. 7 No. 2 February, 2022

International Journal of Mechanical Engineering

Manufacturing time optimization in process route plan development for a front-wheel sub-assembly

Wail Adaileh [1]*

[1]Department of Mechanical Engineering, Tafila Technical University, Tafila 66110, Jordan

Abstract

Process route planning plays an important role in bridging between computer-aided design (CAD) and computer-aided manufacturing (CAM) in modern manufacturing environments. Process route planning aims at defining all machining methods, equipment, tools, and sequence of processes involved in altering the initial stock material into end products according to the CAD designs. The current work develops a time-optimized process route plan to manufacture a front-wheel sub-assembly that contains various materials and a range of simple and complex designs using a computer-aided virtual manufacturing system. Throughout this process route plan, a decision was made to select the most proper process methods, machines, cutting tools, and sequence of machining process to minimize the time and improve the quality of the machined parts. List of machines and corresponding processing parameters were included, and both calculated and actual overall production times were compared and evaluated. The computer-aided virtual manufacturing system optimize the production time focusing on the shortest tool path. The CAD/CAM integration provided a powerful tool to fabricate parts of different levels of complexity. The results of the developed process route plan showed that minimum time and high-quality parts could be achieved.

Keywords: CAD/CAM, Process route planning, Front wheel sub-assembly, Manufacturing, Virtual manufacturing

1. Introduction

The ultimate goal in manufacturing is reducing number of setups, shortening processing time, improving part quality, and minimizing machining cost during a product life cycle [1]. It is highly important to obtain the proper part information to reach the right selection of the desirable manufacturing process and their parameters. Process route planning (process planning) can be used in selecting the most appropriate processes and their sequences given in the CAD design during manufacturing [2,3]. The output of process planning is an operations sheet, which is a document that lists all details of the operations needed to complete the part or assembly without delay [4].

Generally speaking, no two process planners can come up with the same sequence of machining operations. The difficulty raises from several variables that are associated with the process selection [5]. Furthermore, manual process planning requires both skilled process planners and machine tool availability in the shop. To reduce the process planning time and improve production efficiency, computer-assisted process planning (CAPP) approaches are being developed and used [2,6]. However, most existing CAPP systems are developed to generate process plans for certain part types [7]. For instance, some CAPP systems are devoted for producing rotational parts [8,9], whereas other systems [10] are used for prismatic parts. In this work, a manual processing route plan was developed, with the aid of MS-Excel® spread sheets and virtual manufacturing environment (VM) in Creo Parametric® software, to determine the detailed requirements for fabricating the various components of the front wheel sub-assembly prototype used in the SAE formula student vehicle as shown in Figure 1.

2. Front wheel sub-assembly

Front wheel sub-assembly main parts are driving axle hub, brake disc, upright, and steering arm. The hub is connected with the driving axle from one side and with the wheel from the other side to provide the rotational motion to the wheel. The brake disc is responsible for stopping the vehicle by frictional forces with the braking pads. The hollow-shaped disc, shown in Figure 2, was designed to dissipate thermal energy generated due to frictional forces [11]. It is important to mention that the finite element analysis for all parts will not be discussed in the current work. The hub is also directly connected to the upright, which is responsible for connecting all suspension, steering, and braking parts together with the chassis to stabilize the vehicle. Moreover, the upright is connected to the steering arm, allowing the driver to steer the front wheel of the vehicle. Detailed information about different methodologies used to design front wheel sub-assembly components were discussed in Saxena et al. [12]. The design was optimized using computer—aided design and engineering (CAD/CAE) integration in an attempt to reduce the manufacturing time and cost.

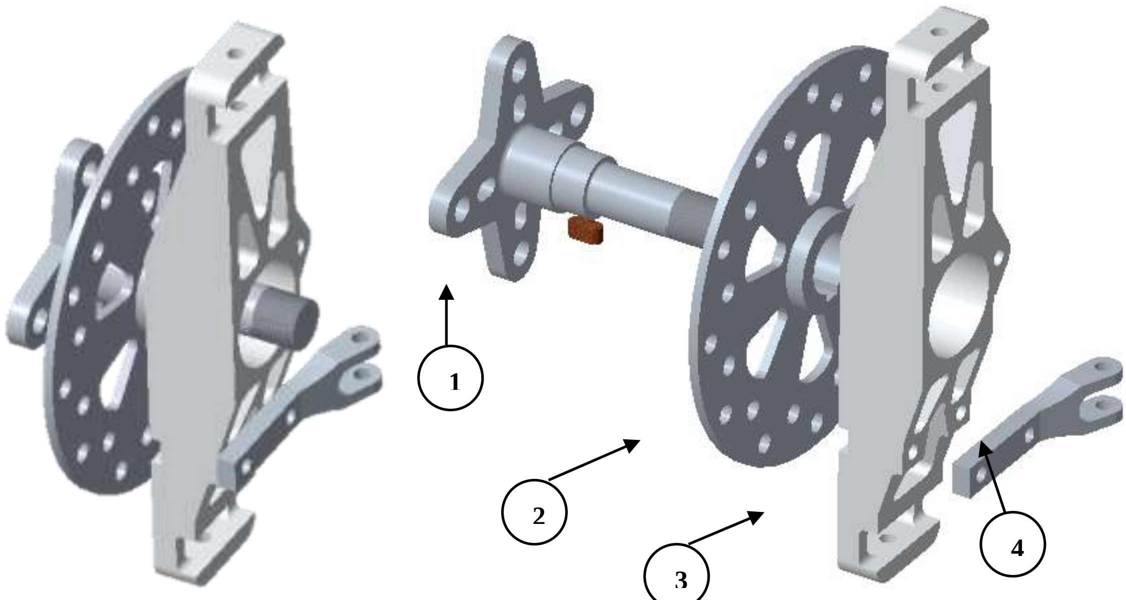

Figure 1: (a) Assembled and (b) exploded views of the front wheel sub-assembly, where 1 is the hub, 2 is the brake disc, three is the upright, and 4 is the steering arm

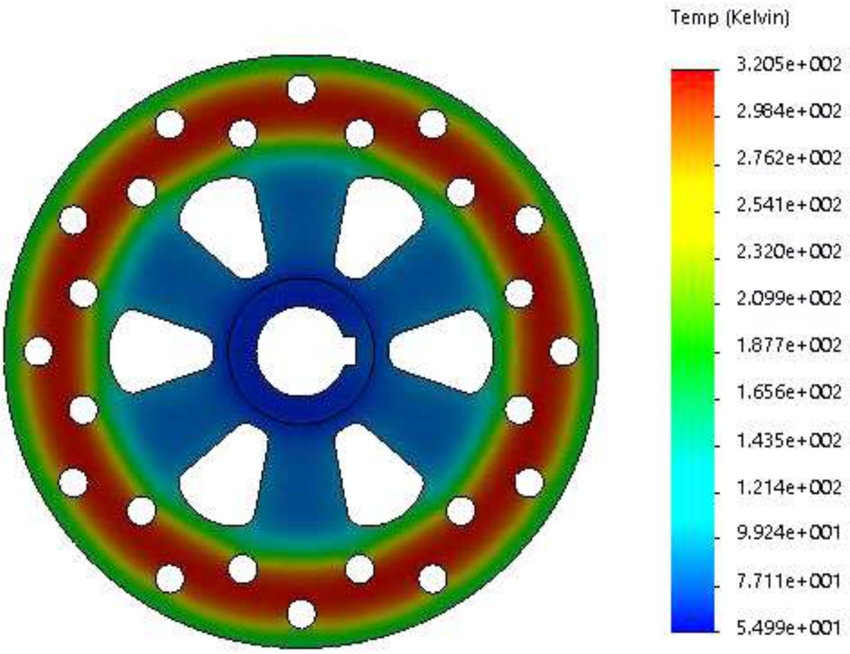

Figure 2: Thermal simulation of the designed brake disc

3. Process route planning

Process route planning was extensively studied and used in several production environments, for instance, in the distributed manufacturing [13] and shop manufacturing systems [14]. The goals of most existing research in this area were focused on one or more conventional management aspect, such as shortest time, minimum machining steps, and lowest cost. The current work is directed towards the selection of the machining methods, equipment, tools, and sequence of machining processes during process route planning.

The importance of process planning stems from its role in combining both product design and manufacturing stages. The basic process planning usually begin during the product design stage, where the selection of materials and their initial forms is established.

Table 1 provides a list of materials and their initial forms and dimensions used in making the front wheel sub-assembly. Furthermore, process route planning takes its inputs from the CAD drawings that indicate what part and how many is to be made. Preliminary decisions about the product to determine which machine, as well as the tools, may be made based on the given drawings [15]. Figure 3 shows the detailed CAD drawings for the front wheel sub-assembly components. The technical knowledge of processes, machines, and tools is required after drawing analysis stage. Table 2 demonstrates the machine codes used in the current study. For each part, a detailed operations sheet is developed.

Table 1: Initial information of the used materials. The part number is corresponding to that in Figure 1.

No.	Part name	Material	Form	Stock dimensions (mm)
1	Hub (2 parts)	AISI 4140	Rod	Ø40 × 125
		AISI 4140	Disc	Ø128 × 10
2	Brake disc	Grey cast iron	Disc	Ø210 × 20
3	Upright	Al 7075-T6	Block	120 × 300 × 50
4	Steering arm	Al 7075-T6	Block	30 × 30 × 120

Table 2: Machine codes and models

Machine	Code	Model (if available)
Arc welding	M01	Miller CST-230
Automatic hex saw	M02	Siloma ON401
CNC milling	M03	San Eagle SHV-850
Drill press	M04	Arboga Sweden
Hydraulic press	M05	N/A
Manual lathe	M06	Mascut MA2160
Waterjet cutting	M07	Easyline 2020

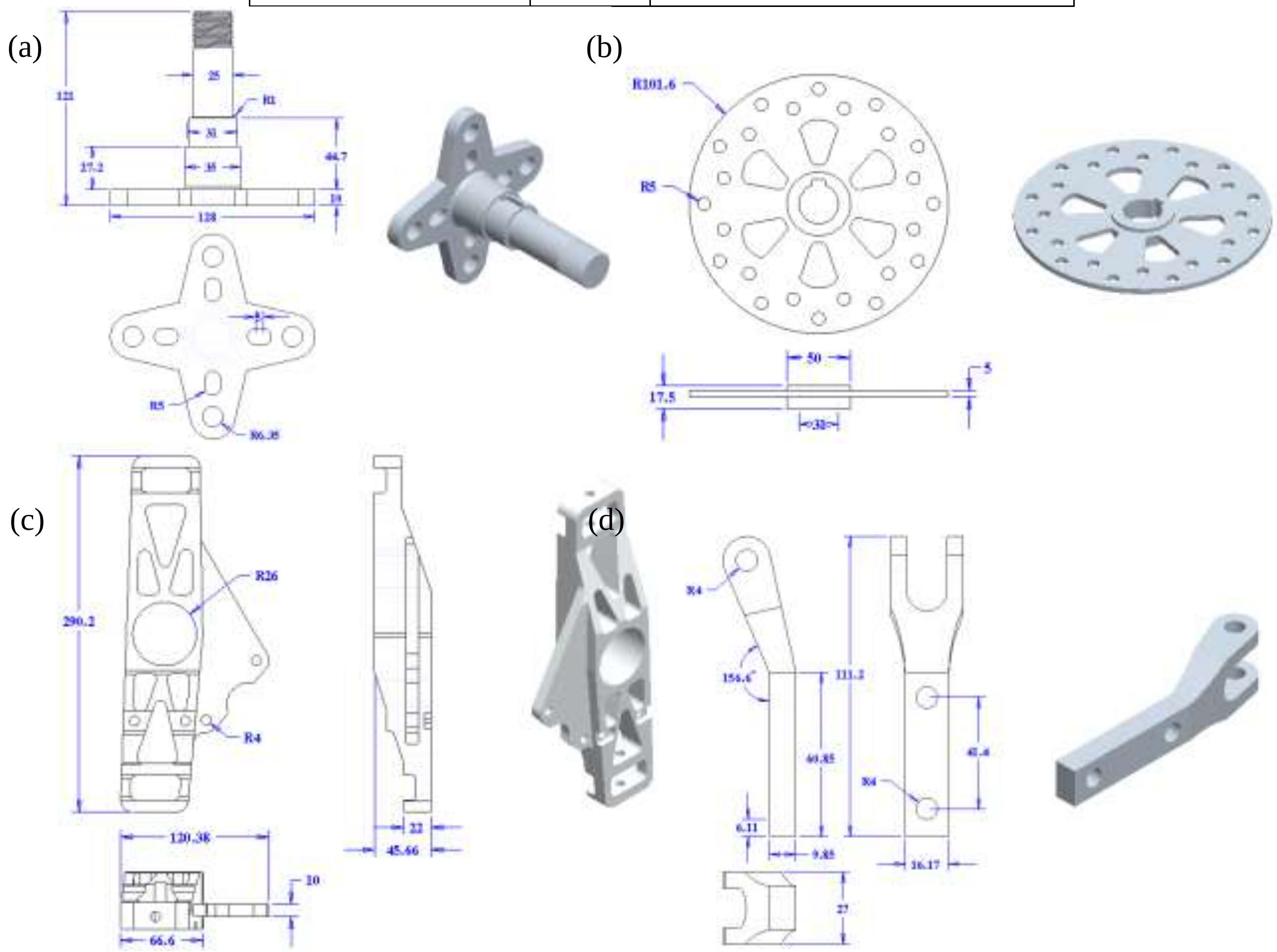

Figure 3: Detailed CAD drawings for the front wheel sub-assembly components. (a) hub, (b) brake disc, (c) upright, and (d) steering arm

3.1 Material selection criteria

The front wheel sub-assembly is naturally subjected to fatigue force, cornering force, braking force, vibration, impact loading, and combination of all forces due to road condition and from the steering movement applied by the driver [12]. Materials with high properties are undoubtedly recommended to secure the driver and the vehicle from any possible failure. Therefore, front wheel sub-assembly components were made from different materials based on the required properties to encounter different loading types. For instance, the hub was made of AISI 4140 steel, which is known for its high strength and toughness. This steel is used in mission-critical structural components because it contains Cr, Mo, and Mn, that improves its hardenability and fatigue resistance [16]. Grey cast iron is the most widely used material for automotive brake discs because of its desirable structure [17], low production cost, and good tribological properties [18]. With flake form of graphite in grey cast iron structure [19], wear and frictional characteristics are highly improved and made it suitable for such application. Grey cast iron is a brittle material and exhibits little plastic deformation when loaded, and thus the yield strength and tensile strengths are almost identical [20]. Both upright and steering arm were made of AISI 7075-T6 aluminum alloy, which is typically used in transport applications, including marine, automotive, and aviation [21]. Typical mechanical properties of AISI 4140 steel and 7075-T6 aluminum alloys are listed in Table 3.

Table 3: Mechanical properties of the selected materials

Material	**σ_T MPa**	**σ_Y MPa**	**E GPa**	**τ MPa**
AISI 4140	655	415	190-210	80
Al 7075-T6	572	503	71.7	331

3.2. Machining processing time (MPT)

It is of high importance to determine the machining operation before calculating the operation actual time. Machining operations used in this work are classified into traditional processes, such as turning, milling, and drilling, and none traditional processes, such as abrasive water jet cutting. The actual machining time was calculated from the equations demonstrated in this section. The time required to perform other operations, such as joining, sawing, and pressing, was estimated using a stop watch.

3.2.1. Turning operations

In surface turning operations, the machining time required to turn a cylindrical part in one pass can be expressed by the following equation [22]:

$$T_t = \frac{\pi D_o L}{f v} \tag{1}$$

where T_t is the turning time, *Do* is the work diameter, mm, *L* is the work length, mm, *f* is the feed, mm/rev, and *v* is the cutting speed, mm/min. The total cutting time is computed based on the number of passes according to the CAD drawing and cutting parameters. In facing turning, the operation is performed in one pass, and the time, T_f, is calculated according to the following equation [23]:

$$T_f = \frac{L_f}{f_f v_f} \tag{2}$$

where L_f is the facing length (radius of the work), mm, f_f is the feed, mm/rev, and v_f is the spindle speed, rev/min.

3.2.2. Milling operations

In the current work, face milling was the main operation used on CNC milling machine. The machining time spent during face milling operation is expressed by [22]:

$$T_m = \frac{L + A_m}{f_r} \tag{3}$$

$$f_r = N . n_t . f \tag{4}$$

$$N = \frac{v}{\pi D} \tag{5}$$

where *L* is the work length, mm, *A* is the cutter approach distance, mm, f_r is the feed rate, mm/min, *N* is the spindle speed, rev/min, n_t is the number of teeth on cutter, *f* is the feed mm/tooth, *v* is the cutting speed, mm/min, and *D* is the cutter diameter, mm. Two possible cases are available to calculate the cutter approach distance based on the cutter position relative to the work. The first case is when the cutter travels from one side to another across the work, the approach distance, A_m, is calculated by:

$$A_m = 0.5\left(D - \sqrt{D^2 - w^2}\right) \tag{6}$$

where *D* is the cutter diameter, mm, and *w* is the part width, mm. The second case is when the cutter is offset to one side of the work; the cutter approach distance is given by:

$$A_m = \sqrt{w(D - w)} \tag{7}$$

The milling time calculations are tedious in most milling operations because of complex part geometry and/or tool path. Under such circumstances, the milling time can be estimated from the material removal rate, R_{MR}, which is determined using the product of the cross sectional area of the cut and the feed rate as follows [22]:

$$R_{MR} = w.d.f_r \quad (8)$$

where *w* and *d* are the width of the work and depth of cut, mm, respectively.

3.2.3. Drilling operations

Drilling operations can be performed by either a drill press machine or by turning on a lathe machine. In both cases, the drilling time, T_d, can be calculated by:

$$T_d = \frac{h + A_d}{f_r} \quad (9)$$

where *h* is the drilling distance, mm and A_d is the drilling approach allowance, mm. The feed rate, f_r, in mm/min is obtained through multiplying the spindle speed, *N*, in rev/min by the feed, *f*, in mm/rev. The drilling approach allowance, A_d, is calculated by:

$$A_d = 0.5D \times tan\left(90 - \frac{\theta}{2}\right) \quad (9)$$

where *D* is the drill diameter, mm, and θ is the drill point angle, degrees. In all machining operations, a small distance was added to the tool path length at the beginning and end of the work to allow for approaching and over travelling. Thus, the duration of the feed motion past the work could be longer than the calculated time. However, this difference was taken into consideration in the current work. It is important to highlight that the same time calculations are used for other related operations to turning, milling and drilling.

When the work is to be machined on several stages, the total machining processing time, *MPT*, can be calculated as:

$$MPT = \sum_{i=1}^{n} t_i \quad (10)$$

where t_i is the processing time of the operation used in stage, *i* and *n* is the process stages in the process route. CNC machining time optimization methods [24] can be classified based on material removal rates [25], NC program and machine characteristics [26], and artificial intelligence methods [27]. The optimization methods based on material removal rates or artificial intelligent are used in rough time estimation due to inadequate information. However, the commercial software calculate the machining time by considering both machining feed rates and length of the tool path, which can give acceptable time accuracy. The NC program and machine characteristics based methods can provide much higher accuracy than other methods. The drawback of this methods is that the machining conditions that influencing the geometry-process information are not taken into account. In order to calculate the machining time accurately, a computer-aided virtual manufacturing system was used in the current work.

4. Virtual manufacturing

Virtual manufacturing (VM) system is a computer system that generates information about the entire manufacturing system similar to these utilized in the real manufacturing environment. In virtual manufacturing, a computer-based environment is generally used to simulate manufacturing processes and the total manufacturing enterprise to optimize the cost, quality, and time of production and to achieve integrated product, process, and resource design [28]. Virtual manufacturing was performed in this work using Creo Parametric® software, which is one of the most sophisticated and advanced solid modelling programs in the market. Solid modeling in Creo Parametric® means that the 3D models contain all the information that a real 3D solid component would contain. The created parts have volumes, which implies that the mass and inertia of the part are known once the material density is provided [29]. Cutting parameters, such as cutting feed, spindle speed, max step depth, step over and tool size, were given to the software in the virtual machining environment based on the material type to predict the actual machining times.

During process route planning, the processes and operations were selected with a great attention on time and quality considerations. The manufacturing cost is definitely of high importance and, more specifically, in manual process route planning optimization. However, the machine, tool, machine change, tool change, and setup change costs were described and used by [2,15] and will not be tackled in the current study.

5. Process parameters

Table 4 lists the typical machining parameters for machining operations [30] based on work and tool materials used in this work. It is important to mention that the table mentions only parameters of the processes used to fabricate the front wheel sub-assembly.

Table 4: Typical parameters for machining operations using high speed steel (HSS) tools

Operation	Work material	Process	v m/min	f mm/rev	d_a mm	d_e mm
Turning	Steel	Turning and facing	D 30 – 40 A 40 - 50	D 0.1– 0.25 A 0.02-0.1	D 0.75-2 A 0.2-0.8	
		Threading	10	Thread pitch		
		Drilling	18	Manual		
		Boring	D 20 – 30 A 30 - 40	D 0.1– 0.25 A 0.02/ 0.1		
	Aluminum	Turning and facing	D 40 – 60 A 60 - 80	D 0.1– 0.25 A 0.02-0.1	D 0.75-2 A 0.2-0.8	
		Threading	15	Thread pitch		
		Drilling	30	Manual		
		Boring	D 30 – 50 A 50 - 70	D 0.1– 0.25 A 0.02-0.1	D 0.75-2 A 0.2-0.8	
Milling	Steel	Face milling	D 20 - 25 A 25 - 30	D 0.05 – 0.1 A 0.01 – 0.05	D 1-2 A 0.2-0.5	~2/3 Ø
	Aluminum		D 50 - 70 A 70 - 90	D 0.05 – 0.1 A 0.01 – 0.05	D 1-2 A 0.2-0.5	~2/3 Ø
Drilling	Steel	Spot drilling	18	0.04 – 0.1		
		Drilling				
	Aluminum	Spot drilling	0.04 – 0.1	0.04 – 0.1		
		Drilling				

***v* = cutting speed, *f* = feed, d_a = axial depth of cut, d_e = radial depth of cut, *D* = roughening and *A*= finishing**

6. Process route planning case study

The front wheel sub-assembly consists of several components that have various complexity levels, as could be concluded from the CAD drawings in Figure 3. Complex shapes require longer manufacturing time as compared to simple shapes. For instance, the upright has many details that make it the most complex and time consuming part in the sub-assembly. These many features require several tool paths. In addition, the job must be rotated in many positions. For mass production, casting is recommended to make the upright. However, it is made by machining in this work because only one piece is required as a prototype. The upright machining was performed on a three axes CNC milling machine that gave us a room to work on other parts while it was machined.

Table 5 is the detailed process route planning for upright manufacturing.

The first step in upright manufacturing process involved removing two 50 × 50 × 50 mm blocks from the initial 120 × 300 × 50 mm Al 7075-T7 block, as shown in Figure 4, by sawing to save time and reduce the scrap amount. The total sawing time was about 20 minutes. During sawing process, the upright CAD drawings were converted into G-code programs and transferred into the CNC milling machine controller.

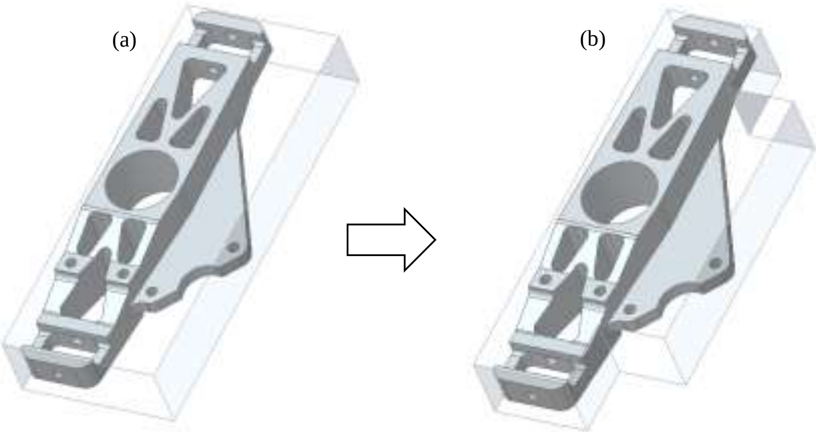

Figure 4: Illustration of the aluminum alloy block preparation for hub manufacturing (a) before and (b) after sawing

Table 5: Details of process planning for hub manufacturing

Part name: **Upright**			Material: **Al 7075-T6**			
Quantity: **1**			Material size: **120 × 300 × 50 mm block**			
Operation	**Machine code**	**Description**	**Tools and Parameters***	**Time (minutes)**		
				Processing	**Tool change**	**Fixture**
Sawing	M06	Removing 50×50×50 mm block	Stop watch	8	0	2
		Removing 50×50×50 mm block	Stop watch	8	0	2
Milling	M03	Figure 5 position 1	EndmillØ10mm	250.3	3	10
		Figure 5 position 2	v =60 m/min	43.6	0	10
		Figure 5 position 3	f_r= 0.35 m/min	21.8	0	10
		Figure 5 position 4	d= 0.5 mm	61.3	0	2
Drilling	M04	Drilling 6 through holes of Ø8 mm	Twist drill bit Ø8mm v= 25 m/min f_r= 0.2 m/min	0.5	2	10
Total machining time (min)						**444.5**

* v is the speed, f_r is the feed rate, and d is the depth of cut

Next, the prepared aluminum alloy block was clamped by a vice mounted on the CNC milling machine bench, as shown in Figure 5 (position 1). A 75 mm long and 10 mm diameter high-speed steel end mill was used in this stage to cut through the job width. Position 1 was suggested to produce the side slopes on the upright smoothly. The same tool was used for other milling operations in positions shown in Figure 5. The total machining time by milling was 412 minutes.

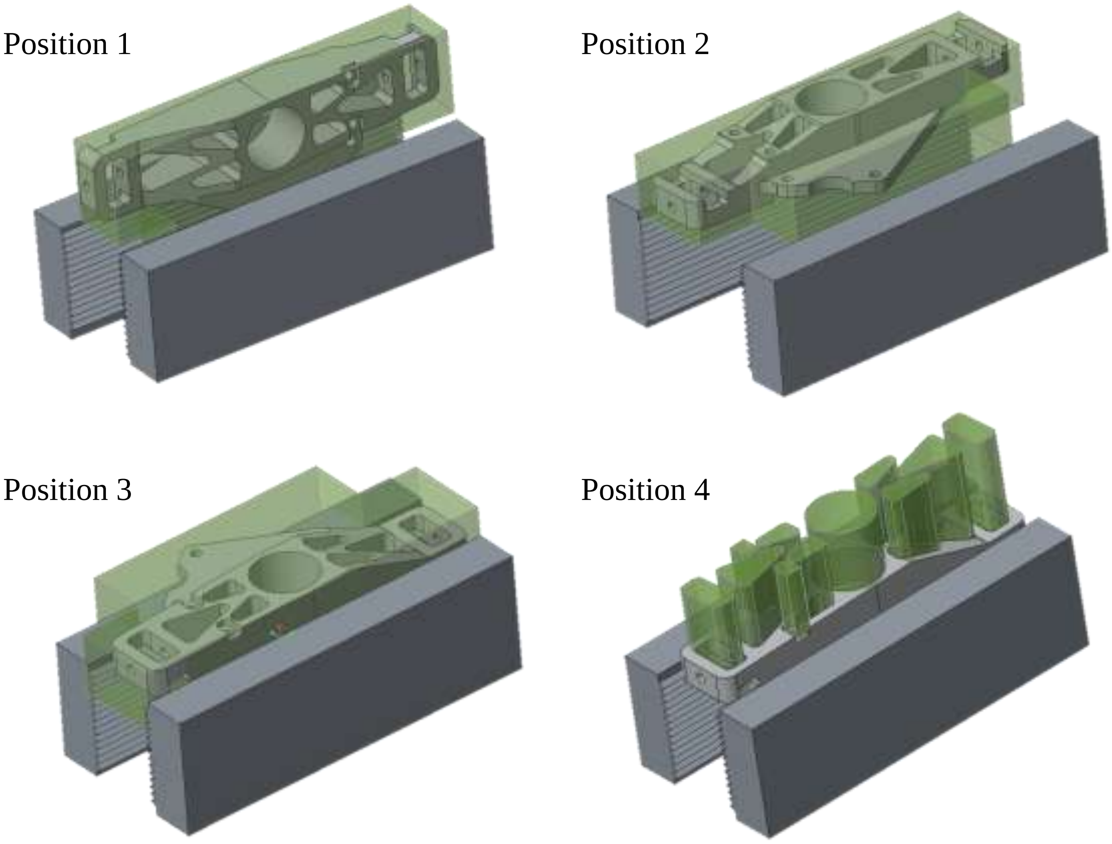

Figure 5: Illustration of different rotation positions of the aluminum alloy block for milling operations. The transparent green features represent the removed material. The positions are corresponding to those in

Table 5.

After sawing and milling, a drilling process was performed using an Ø 8 mm twist drill bit to create six through holes in the upright body. Two holes dedicated to fasten the steering arm (Figure 1), two holes on the thin part (Figure 3c) to fix the brake caliper, and two holes at the top and bottom to connect the upright with the vehicle chassis using tie rods. The total drilling time was about 12.5 minutes. The overall upright manufacturing time was about 444.5 minutes. The upright production timeline is demonstrated in Figure 6.

As mentioned earlier, other parts were processing during the upright machining. It is highly recommended to fabricate the hub as a one-piece component to tolerate different loadings exerted on the front wheel sub-assembly. However, in order to minimize cost, shorten time and reduce scrap amount, the hub was fabricated from two components, i.e., rod and disc. The one-piece component requires about 12 kg AISI 4140 steel rod (Ø120×125 mm) to produce a final product weighing 1.6 kg. This means that about 10.4 kg of the material stock will be wasted as scrap. Furthermore, removing 10.4 kg by machining will be a time consuming and expensive process. The hub fabrication strategy is demonstrated in Table 6.

Figure 7 illustrates the hub stock material preparation, which includes pressing, welding, and turning stages. Both rod and disc were machined using a manual lathe in such a way that the rod is tightly implanted in the disc using a hydraulic press.

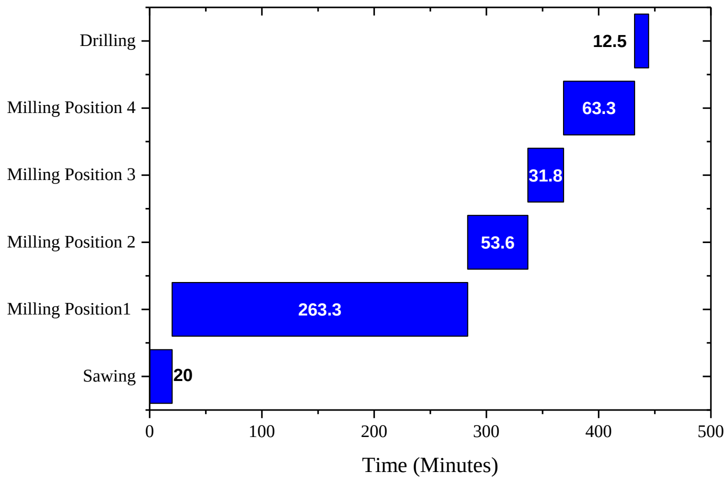

Figure 6: Upright production timeline

The implanted rod was then joined together with the disc using arc welding process. The pressing and welding times were recorded using a stop watch with a total time of 48 minutes. The next turning process was delayed for about 60 minutes in order to allow the weldment to cool down. Typical risk in turning hot components is that the job may fly away from the machine chuck when it cools down due to metal shrinking. Such conditions may result in deadly accidents and big economical losses. One may suggest to quench the job in cold water to expedite the process. In fact, the job was not quenched and left to cool down slowly to reduce the hardness that may result from the welding process. AISI 4140 steel is highly susceptible to cracking after welding because of excessive grain growth and the formation of non-tempered martensite with a high hardness levels in the heat affected zone (HAZ) [31]. Thus, cooling in still air is considered a post-welding heat treatment to avoid metallurgical problems.

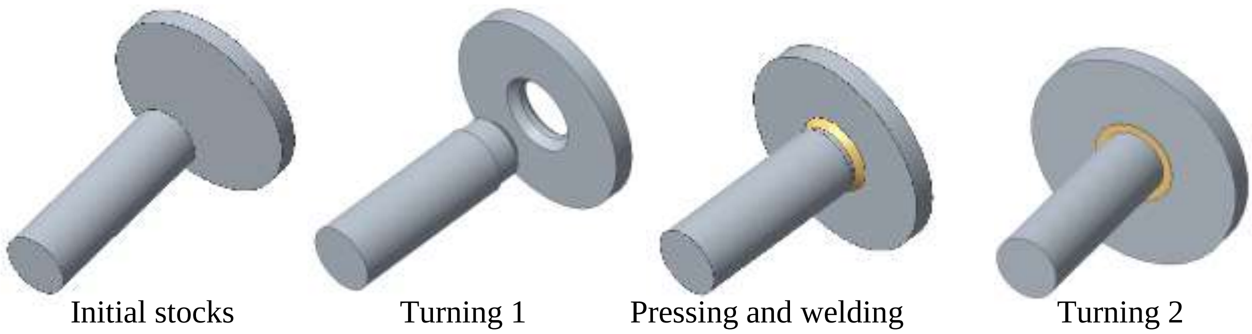

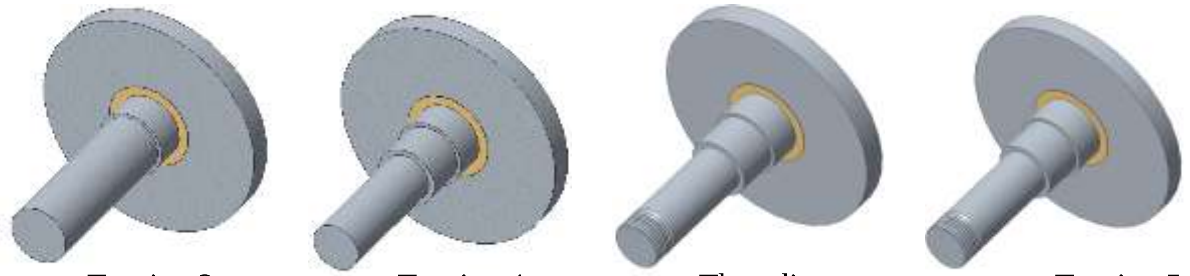

Figure 7: Illustration of the hub stocks preparation, pressing, welding, and turning stages. The golden area represents the welding line. The stages are corresponding to those in Table 6.

It is important to mention that the rod finishing pass parameters were not included in the process route planning when the bearing size of Ø25 mm was made. However, the time was compensated in Table 6 near Turning 4 operation. The machining parameters used for finishing pass, when Ø25 mm bearing size was made, are the cutting speed $\boldsymbol{v}$ = 150 m/min, feed rate $\boldsymbol{f_r}$ = 0.1 mm/rev, depth of cut $\boldsymbol{d}$ = 0.05 mm. These parameters were also recommended by [32]. The finishing pass took around 2.3 minutes to reduce the rod diameter to 25.05 mm.

Three milling operations were scheduled to complete the hub manufacturing. Figure 8 demonstrates the milling operation features. The total time required for hub machining by milling was about 130 minutes. While the hub was operated by milling, the brake disc stock material was machined on the lathe to prepare the disc for the subsequent water jet cutting process. Table 7 demonstrates the details of the disc brake process route plan. The hub production timeline is demonstrated in Figure 9.

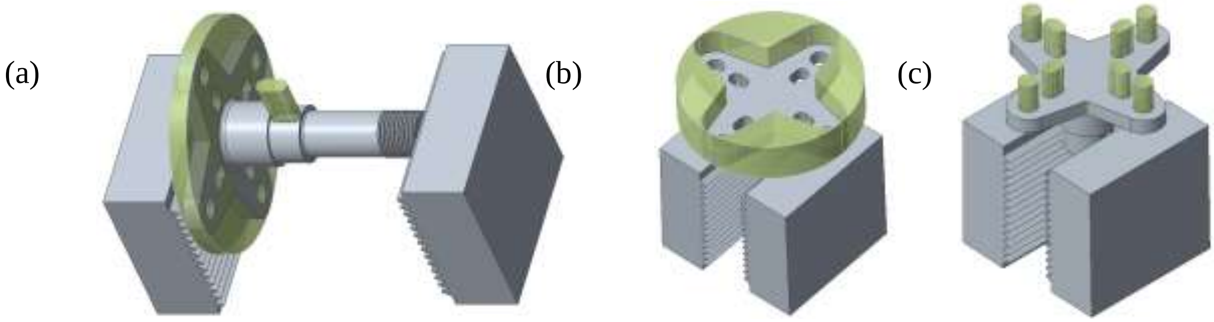

Figure 8: Illustration of the hub milling operations. The transparent green features represent the removed material.

Table 6: Details of process planning for hub manufacturing

<table>
<tr><td colspan="3">Part name: Hub</td><td colspan="4">Material: AISI 4140</td></tr>
<tr><td colspan="3">Quantity: 1</td><td colspan="4">Material size: Ø40×125 mm rod
Ø128×12 mm disc</td></tr>
<tr><th rowspan="2">Operation</th><th rowspan="2">Machine code</th><th rowspan="2">Description</th><th rowspan="2">Tools and Parameters</th><th colspan="3">Time (minutes)</th></tr>
<tr><th>Processing</th><th>Tool change</th><th>Fixture change</th></tr>
<tr><td>Turning 1</td><td>M06</td><td>Rod turning to Ø37×20 mm</td><td rowspan="2">Single point cutting tool and Ø35mm twist drill
v =80 m/min
f_r= 0.1 m/min
d= 0.3 mm</td><td>1.5</td><td>3</td><td>0</td></tr>
<tr><td></td><td>M06</td><td>Disc boring to Ø37×10 mm</td><td>5</td><td>5</td><td>0</td></tr>
<tr><td>Pressing</td><td>M05</td><td>Pressing the rod and the disc</td><td>Stop watch</td><td>10</td><td>0</td><td>3</td></tr>
<tr><td>Welding</td><td>M01</td><td>Welding the rod to the disc</td><td>Stop watch</td><td>30</td><td>0</td><td>5</td></tr>
<tr><td>Turning 2</td><td>M06</td><td>Rod turning to Ø35×111 mm</td><td rowspan="5">Single point cutting tool
v =80 m/min
f_r= 0.1 m/min
d= 0.3 mm</td><td>3.4</td><td>60</td><td>0</td></tr>
<tr><td>Turning 3</td><td>M06</td><td>Rod turning to Ø31×83.8 mm</td><td>4.6</td><td>0</td><td>0</td></tr>
<tr><td>Turning 4</td><td>M06</td><td>Rod turning to Ø25×66.3 mm</td><td>4.4+2.3</td><td>0</td><td>0</td></tr>
<tr><td>Threading</td><td>M06</td><td>Rod Threading M25×21 mm</td><td>12</td><td>3</td><td>0</td></tr>
<tr><td>Turning 5</td><td>M06</td><td>Disc turning to Ø128×10 mm</td><td>0.8</td><td>3</td><td>0</td></tr>
<tr><td>Milling 1</td><td>M03</td><td>Key way 17.5×8×4 mm</td><td rowspan="3">End mill
Ø8mm
v =50 m/min</td><td>4</td><td>0</td><td>6</td></tr>
<tr><td>Milling 2</td><td>M03</td><td>Figure 8 (b)</td><td>74</td><td>0</td><td>4</td></tr>
<tr><td>Milling 3</td><td>M03</td><td>Figure 8 (c)</td><td>42</td><td>0</td><td>0</td></tr>
</table>

			f_r= 0.15 m/min d= 0.2 mm			
Total machining time (min)						**286**

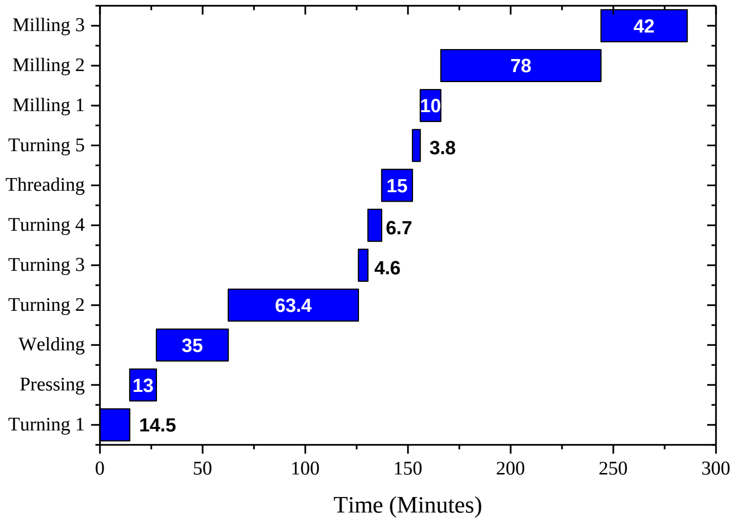

Figure 9: Hub production timeline

The grey cast iron disc thickness was reduced by turning from 20 mm to 17.5 mm. 1.25 mm was removed from each face. After this stage, both disc surfaces are guaranteed to be parallel. The disc CAD drawing was converted to DXF format and fed to the water jet controller. The cutting profile is presented in Figure 3b. The total processing time by water jet was about 45 minutes. Water jet cutting operation was used because it is relatively very fast process, environmentally friendly and the dimensions of the cut features are less important. Furthermore, it was easy to cut the key way. Figure 10 demonstrates the disc brake manufacturing operations. Grey cast iron corrodes when contacted with water, as could be observed after cutting. However, the rust layer was removed by subsequent machining processes. It is important to mention that disc brake is often in contact with water during its service due to road and washing fluids. But the rust layer is always removed by friction with the breaking pads [18].

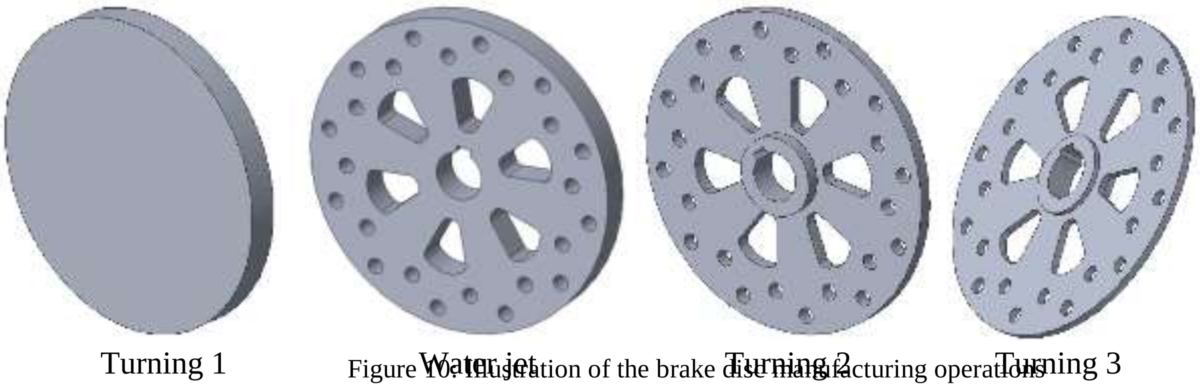

Figure 10: Illustration of the brake disc manufacturing operations

Table 7: Details of process planning for brake disc manufacturing

Part name: **Brake disc**			Material: **Grey cast iron**			
Quantity: **1**			Material size: **Ø210×30 mm**			
Operation	**Machine code**	**Description**	**Tools and Parameters**	**Time (minutes)**		
				Processing	**Tool change**	**Fixture change**
Turning 1	M06	Turning 1.25 mm from the face	Single point cutting tool v =120 m/min f_r= 0.3 m/min d= 0.5 mm	5	0	5
		Turning 1.25 mm from the face		5	0	2
Water jet	M07	Figure 3b	NC program	45	0	7
Turning 2	M06	Removing 9 mm form thickness and diameter down to 50 mm	Single point cutting tool v =120 m/min f_r= 0.3 m/min	36	0	2
Turning 3	M06	Removing 3.5 mm form thickness and diameter down to		14	0	5

		50 mm	d= 0.5 mm			
Total machining time (min)						**126**

After water jet cutting, the disc was chucked at its outer diameter, and 9 mm from the surface thickness were removed by turning the diameter down to 50 mm. This step was intestinally processed to create an edge for adequate gripping when other side of the disc is machined. However, the drawback of this step is that the fixture change time increased because the chuck gripping size must be adjusted to 50 mm from 210 mm in the previous step. The other side of the disc was machined down to 50 mm diameter, and 3.5 mm were removed from the thickness. The total manufacturing time of the brake disc was about 126 minutes. The brake disk production timeline is demonstrated in Figure 11.

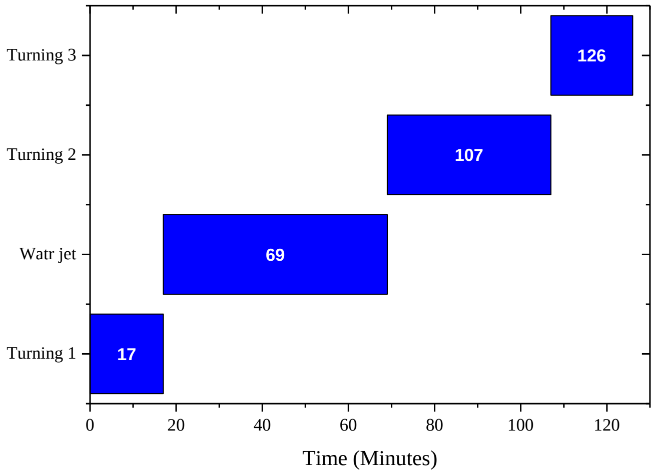

Figure 11: Brake disc production timeline

The steering arm was made from 7075-T6 aluminum alloy because of its desired mechanical properties, as discussed earlier. Same milling parameters to those used in the upright fabrication were adapted for steering arm machining. The steering arm was manufactured by milling using three gripping positions, as shown in Figure 12. In Position 1, the part was clamped on the complex shape of the part in order to establish a new parallelogram base for subsequent milling operations. The depth of cut in these operations was reduced to 0.25 mm to avoid excess pressure on the part and vibration because of its small geometry. The total machining time was about 134 minutes. The steering arm production timeline is demonstrated in Figure 13.

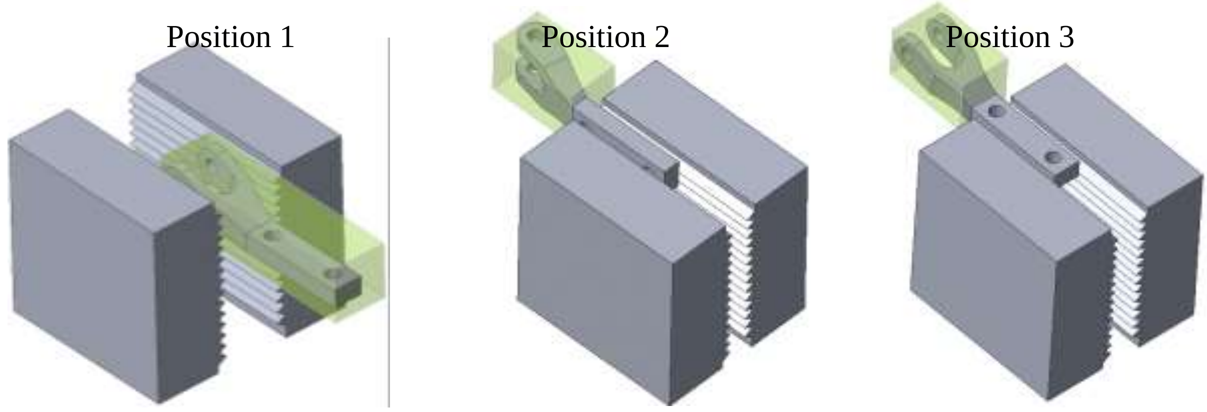

Figure 12: Illustration of the steering arm milling operations. The transparent green features represent the removed material.

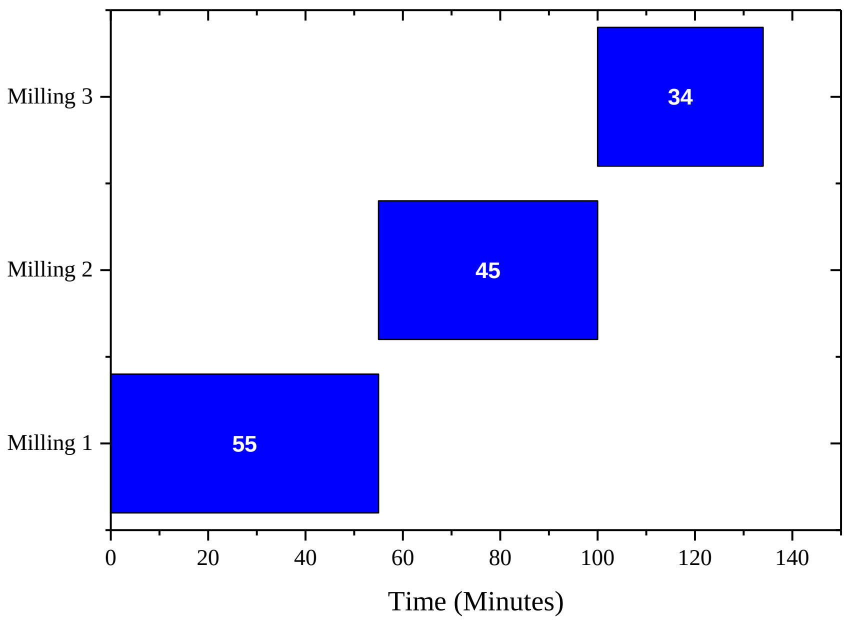

Figure 13: Steering arm production timeline

Table 8: Details of process planning for hub manufacturing

Part name: **Upright**			Material: **Al 7075-T6**			
Quantity: **1**			Material size: **120 × 300 × 50 mm block**			
Operation	**Machine code**	**Description**	**Tools and Parameters**	**Time (minutes)**		
				Processing	**Tool change**	**Fixture**
Milling 1	M03	Figure 12 (Position 1)	End mill Ø8mm	51	0	4
Milling 2	M03	Figure 12 (Position 2)	v =60 m/min	41	0	4
Milling 3	M03	Figure 12 (Position 3)	f_r= 0.35 m/min d= 0.25 mm	30	0	4
Total machining time (min)						**134**

In all virtual milling operations, the shortest tool path was adopted to minimize the manufacturing time. For instance, Figure 14 shows two different tool paths that can be assumed to machine the hub disc. Figure 14 (a) is called TYPE_3 scan type, which gives around 74 minutes for overall milling operation. Whereas, Figure 14 (b), so called TYPE_SPIRAL scan type, gives 5 minutes longer milling operation than that in TYPE_3. Same strategy was followed for milling operations of other parts.

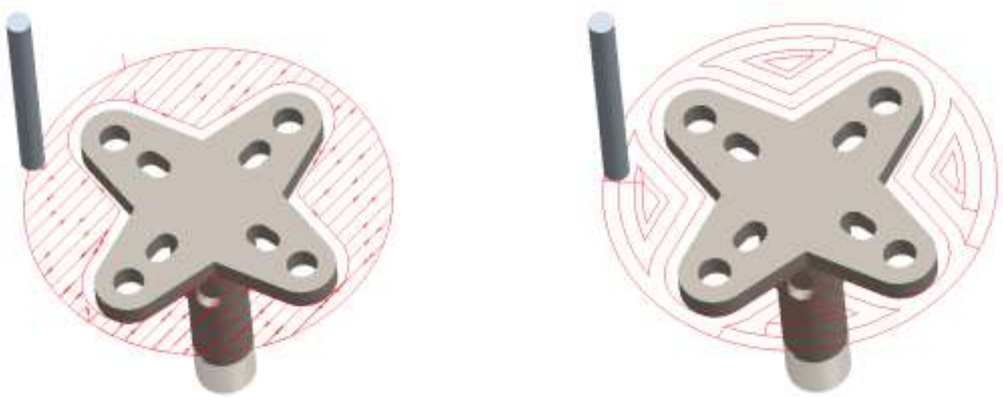

Figure 14: Examples of different tool paths for hub milling two operation. (a) TYPE_3 scan type and (b) TYPE_SPIRAL scan type

The manufactured parts were then manually deburred using a set of files with different sizes and shapes. After each process, the parts were measured to assure that the actual part geometry meets with the CAD designs. The front wheel components were assembled together, as shown in Figure 15. The assembly process took around 30 minutes, which were added to the total manufacturing time to become 1020.5 minutes (17 hours), in case the parts were manufactured consequently. In fact, the calculated time assumes that all parts are made without any delay, which is not the case here. Some operations were impossible to run when other machines were busy.

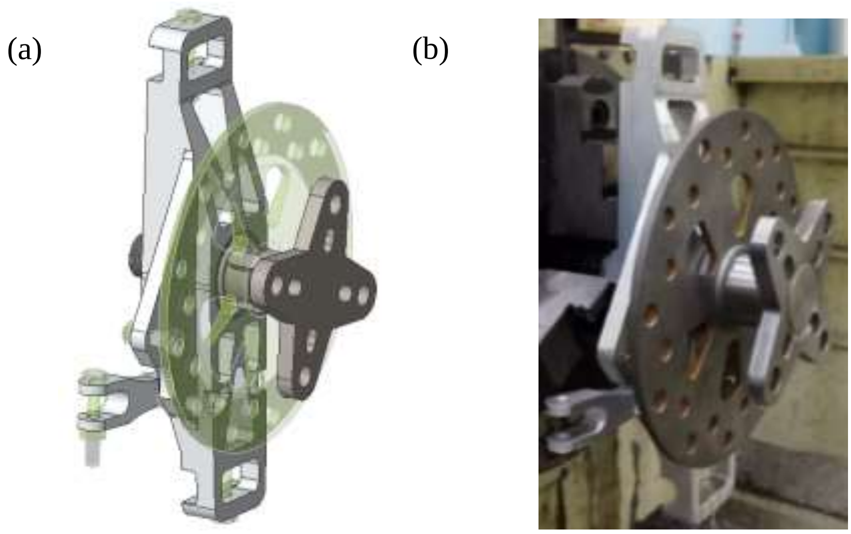

Figure 15: Front wheel sub-assembly. (a) CAD design and (b) actual design

The calculated manufacturing time with machine delays is summarized in Figure 16. Because of the long occupation time of the upright on the milling machine, other milling processes were delayed for about 412 minutes before they begin. However, with all delays, the calculated overall manufacturing time was 676 minutes (11.26 hours), in case the parts were manufactured simultaneously.

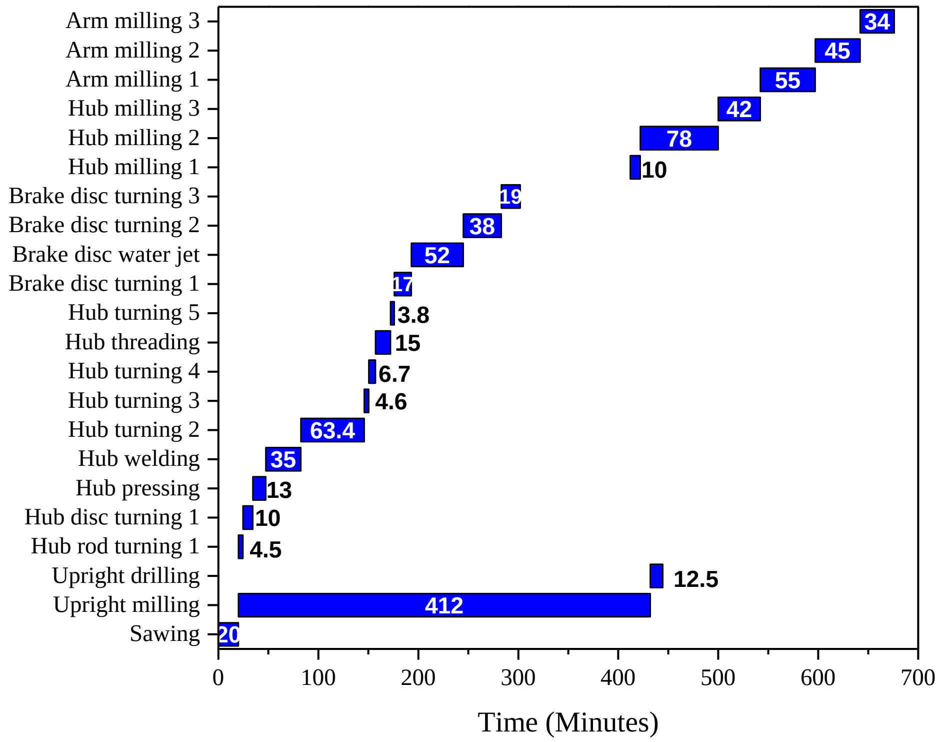

Figure 16: Overall timeline for front wheel sub-assembly production

7. Conclusions

In this work, a process route planning sheet for front wheel sub-assembly components was developed, and the processing time was optimized using a computer-aided virtual manufacturing system. In most cases, the calculated times in minutes were rounded to the nearest integer to ease counting. The overall calculated manufacturing time, considering delays, shortest tool paths, and simultaneous production, was about 676 minutes (11.26 hours), which is less than the actual time. The actual manufacturing time was about 1,320.0 minutes (22 hours) due to some technical issues, such as machine cleaning, machine warming up, changing oils, and others. The upright manufacturing was the longest operation because it was made by machining. Metal casting is recommended for making the upright in case of mass production. The water jet cutter was used because it is environmentally friendly process in the first place, although a CNC milling machine was available. For future work, the overall manufacturing time could be shortened by using special cutting tools, such as cemented carbide and cobalt-coated tools, which can be operated at higher cutting speeds and feed rates.

In turning As a practical matter, a small distance is usually added to the workpart length at the beginning and end of the piece to allow for approach and over travel of the tool. Thus, the duration of the feed motion past the work will be longer than Tm.

8. Acknowledgment

Authors of the current work thank Tafila Technical University for the financial support. Thanks are also extended to Mr. Amer Al Alamayreh for his help in granting access to the CAD/CAM laboratory and operating the machines. Authors would also acknowledge the efforts of Formula Student project team for their valuable contributions.

References

[1] Q. Yi, C. Li, X. Zhang, F. Liu, Y. Tang, An optimization model of machining process route for low carbon manufacturing, Int. J. Adv. Manuf. Technol. 80 (2015) 1181–1196. doi:10.1007/s00170-015-7064-8.

[2] O. Al-Shebeeb, B. Gopalakrishnan, Computer Aided Process Planning Approach for Cost Reduction and Increase in Throughput, in Int. Conf. Ind. Eng. Oper. Manag., Detroit, Michigan, USA, n.d.: pp. 632–644.

[3] M.R. Henderson, G.J. Chang, FRAPP: Automated feature recognition and process planning from solid model data, in Comput. Eng. 1988 - Proc., Publ by American Soc of Mechanical Engineers (ASME), New York, NY, United States, 1988: pp. 529–536.

[4] P.M. Swamidass, PROCESS PLANNING, in Encycl. Prod. Manuf. Manag., Springer US, n.d.: pp. 552–553. doi:10.1007/1-4020-0612-8_721.

[5] R. Meenakshi Sundaram, Process planning and machining sequence, Comput. Ind. Eng. 11 (1986) 184–188. doi:10.1016/0360-8352(86)90075-6.

[6] L.-H. Qiao, Z.-B. Yang, H.-P. Ben Wang, A computer-aided process planning methodology, Comput. Ind. 25 (1994) 83–94. doi:10.1016/0166-3615(94)90035-3.

[7] D.K. Jeba Singh, C. Jebaraj, Feature-based design for process planning of machining processes with optimization using genetic algorithms, Int. J. Prod. Res. 43 (2005) 3855–3887. doi:10.1080/00207540500032160.

[8] T. Gupta, An expert system approach in process planning: Current development and its future, Comput. Ind. Eng. 18 (1990) 69–80. doi:10.1016/0360-8352(90)90042-K.

[9] B.J. Davies, I.L. Darbyshire, The Use of Expert Systems in Process-Planning, CIRP Ann. 33 (1984) 303–306. doi:10.1016/S0007-8506(07)61431-0.

[10] H. Eskicioglu, B.J. Davies, An Interactive Process Planning System for Prismatic Parts (ICAPP), CIRP Ann. 32 (1983) 365–370. doi:10.1016/S0007-8506(07)63422-2.

[11] M. Bouchetara, A. Belhocine, M. Nouby, D.C. Barton, A. Bakar, Thermal analysis of ventilated and full disc brake rotors with frictional heat generation, Appl. Comput. Mech. (2014).

[12] G. Saxena, A.S. Chauhan, R. Jain, I. Gupta, Simulation and Optimization of wheel Hub and Upright of Vehicle: A Review, IOSR J. Mech. Civ. Eng. 14 (2017) 42–50. doi:10.9790/1684-1401034250.

[13] L. Li, J.Y.H. Fuh, Y.F. Zhang, A.Y.C. Nee, Application of genetic algorithm to computer-aided process planning in distributed manufacturing environments, Robot. Comput. Integr. Manuf. 21 (2005) 568–578. doi:10.1016/j.rcim.2004.12.003.

[14] X. Shao, X. Li, L. Gao, C. Zhang, Integration of process planning and scheduling—A modified genetic algorithm-based approach, Comput. Oper. Res. 36 (2009) 2082–2096. doi:10.1016/j.cor.2008.07.006.

[15] R. Kesavan, C. Elanchezhian, B. Ramnath, Process Planning and Cost Estimation, 2nd ed., New Age International Publishers, New Delhi, India, 2009.

[16] V. Nagarajan, S. Putatunda, J. Boileau, Fatigue Crack Growth Behavior of Austempered AISI 4140 Steel with Dissolved Hydrogen, Metals (Basel). 7 (2017) 466. doi:10.3390/met7110466.

[17] J. Machuta, I. Nová, Metallurgy of the Grey Cast Iron for the Automotive Parts, Metallofiz. I NOVEISHIE TEKHNOLOGII. 39 (2017) 1267–1279. doi:10.15407/mfint.39.09.1267.

[18] A. Polak, J. Grzybek, The mechanism of changes in the surface layer of grey cast iron automotive brake disc, Mater. Res. 8 (2005) 475–479. doi:10.1590/S1516-14392005000400020.

[19] D.E. Krause, Gray Iron—A Unique Engineering Material, in Gray, Ductile, Malleable Iron Cast. Capab., ASTM

International, West Conshohocken, PA, 1969: pp. 3–28. doi:10.1520/STP47366S.

[20] E.P. DeGarmo, J.T. Black, R.A. Kohser, Materials and processes in manufacturing, 9th ed., John Wiley & Sons Inc., 2003.

[21] J.R. Davis, Aluminum and Aluminum Alloys, Light Met. Alloy. (2001). doi:10.1361/autb2001p351.

[22] M.P. Groover, Fundamentals of modern manufacturing : materials, processes, and systems, J. Wiley & Sons, Hoboken, USA, 2007.

[23] M.G.A. Kassir, M.M.H. Al-Khafaji, H.L. Alwan, Computing Cutting Time in Turning Operation Based on AutoCAD Drawings ., in 1stRegional Conf. Eng. Sci. NUCEJ Spat. ISSUE, 2008.

[24] B.R. Borkar, M. Kuthe, S. Deshpande, Optimization of Machining Time using Feature Based Process Planning, 2014.

[25] C. Ou-Yang, T.S. Lin, Developing an integrated framework for feature-based early manufacturing cost estimation, Int. J. Adv. Manuf. Technol. 13 (1997) 618–629. doi:10.1007/BF01350820.

[26] H. Siller, C.A. Rodriguez, H. Ahuett, Cycle time prediction in high-speed milling operations for sculptured surface finishing, J. Mater. Process. Technol. 174 (2006) 355–362. doi:10.1016/j.jmatprotec.2006.02.008.

[27] H.R. Maier, G.C. Dandy, Neural network based modelling of environmental variables: A systematic approach, Math. Comput. Model. 33 (2001) 669–682. doi:10.1016/S0895-7177(00)00271-5.

[28] J.A. Burt, DoD Guide to Integrated Product and Process Development (Version 1.0), Washington, DC, 20301-3000, 1996.

[29] P.O. Kanife, Computer Aided Virtual Manufacturing Using Creo Parametric, Springer International Publishing, Cham, 2016. doi:10.1007/978-3-319-23359-8.

[30] E. Oberg, F. Jones, H. Horton, H. Ryffel, C. McCauley, Machinery's handbook, 30th ed., Industrial Press, Connecticut, USA, 2016.

[31] C.C. Silva, V.H.C. de Albuquerque, C.R.O. Moura, W.M. Aguiar, J.P. Farias, Evaluation of AISI 4140 Steel Repair Without Post-Weld Heat Treatment, J. Mater. Eng. Perform. 18 (2009) 324–331. doi:10.1007/s11665-008-9294-5.

[32] A. Hamdan, A.A.D. Sarhan, M. Hamdi, An optimization method of the machining parameters in high-speed machining of stainless steel using coated carbide tool for best surface finish, Int. J. Adv. Manuf. Technol. 58 (2012) 81–91. doi:10.1007/s00170-011-3392-5.